

**Are your MRI contrast agents cost-effective?**

Learn more about generic Gadolinium-Based Contrast Agents.



**AJNR**

**Feasibility of Angiographic CT in  
Peri-Interventional Diagnostic Imaging: A  
Comparative Study with Multidetector CT**

M.-N. Psychogios, J.-H. Buhk, P. Schramm, A. Xyda, A.  
Mohr and M. Knauth

This information is current as  
of April 17, 2024.

*AJNR Am J Neuroradiol* 2010, 31 (7) 1226-1231

doi: <https://doi.org/10.3174/ajnr.A2086>

<http://www.ajnr.org/content/31/7/1226>

ORIGINAL  
RESEARCH

M.-N. Psychogios

J.-H. Buhk

P. Schramm

A. Xyda

A. Mohr

M. Knauth



# Feasibility of Angiographic CT in Peri-Interventional Diagnostic Imaging: A Comparative Study with Multidetector CT

**BACKGROUND AND PURPOSE:** The ability to perform neuroimaging on the angiography suite is important in making decisions during neurointerventions. Our aim was the evaluation of ACT as a fast available diagnostic tool during and after neuroendovascular procedures and the comparison of ACT with postinterventional MDCT.

**MATERIALS AND METHODS:** Eighty-four peri-interventional ACT acquisitions were obtained and evaluated: 38 after coil embolization of cerebral aneurysms, 16 after intracranial angioplasty with stent placement, and 30 after endovascular mechanical thrombectomy and lysis. Interventions and ACTs were performed on a biplane angiography system equipped with flat panel detectors. Postprocessing was performed on a dedicated workstation, and multiplanar reformations were generated. Reference studies were performed on a 16- or 128-section MDCT scanner. All studies were independently evaluated by 3 blinded neuroradiologists. The Wilcoxon test was applied for the statistical analysis.

**RESULTS:** ACT and MDCT images were of equal diagnostic quality in most cases related to the supratentorial ventricular system and the detection of hemorrhages (subarachnoidal, intraparenchymal, and intraventricular). Regarding the supratentorial ventricular system, an adequate diagnostic quality was assigned to 94% of the ACT acquisitions. For the detection of hemorrhage, no statistically significant difference was noted between ACT and MDCT. However, for the infratentorial region, ACT performed relatively poorly compared with MDCT. The diagnostic evaluation of gray matter (basal ganglia, insular cortex, and central cortex) by ACT is not sufficient, with <20% of the acquisitions scoring a diagnostic value.

**CONCLUSIONS:** After neuroendovascular procedures and within the angiography suite, ACT enables an immediate detection of peri-interventional hemorrhage or hydrocephalus. However, for the detection of cerebral infarction, ACT is not yet reliable.

**ABBREVIATIONS:** ACT = angiographic CT; CTDI<sub>w</sub> = weighted CT dose index; DSA = digital subtraction angiography; EVD = external ventricular drainage catheter; HU = Hounsfield unit; ICH = intracerebral hemorrhage; IPH = intraparenchymal hemorrhage; IVH = intraventricular hemorrhage;  $\kappa_w$  = weighted  $\kappa$ ; MDCT = multidetector CT; MPR = multiplanar reformations; SAH = subarachnoidal hemorrhage; ST = section thickness

Flat panel detector—equipped angiography systems provide a new method of volume imaging called ACT or flat panel volume CT. This method enables the CT-like assessment of soft-tissue structures.<sup>1</sup> Contrary to 3D rotational angiography, which is primarily a technique to visualize high-contrast targets like contrast-enhanced intracranial vessels, ACT produces CT-like images of low-contrast tissues such as the cerebral parenchyma, contributing to the detection of potential complications like hemorrhage or hydrocephalus during or directly after the intervention, within the angiography suite.<sup>2</sup> ACT is a method based on the development and use of flat panel detectors in angiographic devices, providing much higher acquisition speed and image-information attenuation

than formerly used image-intensifier-equipped systems.<sup>3</sup> Furthermore, ACT provides a CT-like contrast resolution allowing the depiction of objects down to 10 HU of attenuation difference.<sup>4–6</sup> The spatial resolution can be even higher than that in current MDCT examinations with an isotropic resolution of <0.1 mm.<sup>7</sup> Also, ACT, being a volume dataset of approximately 20-cm width and 25-cm height, can be applied for 3D and MPR in the same way as a spiral CT dataset. All these technical aspects of ACT make it an application of potentially great importance during or after neurointerventional procedures.<sup>8–10</sup>

In our study, we included 84 ACTs acquired on a biplane angiography scanner, during or immediately after a neuroendovascular procedure, in the period of 2006–2009. The purpose of our study was to evaluate the feasibility and diagnostic value of ACT in peri-interventional imaging and, particularly, in the detection and progress of hemorrhage or hydrocephalus. In addition, we aimed to evaluate the differentiation of gray and white matter, trying to observe if there is a capability to perform stroke imaging within the angiography suite. The ACTs were scored on a 3-point scale and statistically compared with postinterventional MDCT images obtained di-

Received November 24, 2009; accepted after revision January 29, 2010.

From the Department of Neuroradiology, (M.-N.P., P.S., A.X., A.M., M.K.) University Medicine Goettingen, Goettingen, Germany and Department of Diagnostic and Interventional Radiology (J.-H.B.), University Hospital Hamburg-Eppendorf, Hamburg, Germany.

Paper previously presented at: Annual Meeting of the European Congress of Radiology, March 7–11, 2008; Vienna, Austria; preliminary results after 40 cases.

Please address correspondence to M.N. Psychogios, MD, Department of Neuroradiology, University Medicine Goettingen, Robert Koch 40, 37075, Goettingen, Germany; email: m.psychogios@med.uni-goettingen.de

DOI 10.3174/ajnr.A2086



**Fig 1.** A, A 51-year-old man with a symptomatic middle cerebral artery stenosis. B, After percutaneous transluminal angioplasty and application of a Wingspan stent (Boston Scientific, Natick, Massachusetts), DSA depicts the successful vessel reconstruction. C, Stent conformity and deployment are displayed on 3D reconstructions after postprocessing the same volume dataset that provided us with the ACT. The postinterventional ACT (D) shows an SAH and contrast-agent accumulation primarily in the right lateral sulcus. MDCT (E) verifies this finding. The supratentorial ventricular system can be sufficiently evaluated in both examinations. The old right anterior cerebral artery infarction can be diagnosed on MDCT (E) but is undetectable on the ACT examination (D). F, Follow-up MDCT after 3 days shows complete resolution of SAH.

rectly after the procedure or in a time period of 4 hours after the intervention.

## Materials and Methods

### Patients

Between November 2006 and May 2009, 84 patients (51 women, 33 men; age range, 32–73 years; median age, 63 years) underwent a neuroendovascular procedure in our department. Coil embolization of ruptured cerebral aneurysms was performed in 38 patients. Sixteen patients underwent an intracranial angioplasty with stent placement, and 30, an endovascular mechanical thrombectomy and lysis. In most patients with ruptured aneurysms and SAH, an EVD was applied before the endovascular procedure. ACT was performed to rule out any peri-interventional complications such as hemorrhage or hydrocephalus, to confirm the exact position of the EVD but also to diagnose possible signs of cerebral infarction or edema.

Approval of the local ethics committee was obtained.

### Image Acquisition

Neuroendovascular procedures and ACTs were performed on a biplane angiography system equipped with flat panel detectors (Axion Artis dBA; Siemens, Forchheim, Germany). For the ACT acquisition, we used the DynaCT program (Siemens) in our suite with the

following parameters: 20 seconds of rotation; 538 projections; 220° total angle; CTDI<sub>w</sub>, approximately 35 mGy (manufacturer's information); 30 × 40 cm detector, which allows the reconstruction of a nontruncated volume of approximately 22 cm (in-plane) and 16 cm (in the z-direction). Conventional multislice CT scans were obtained within 4 hours after the intervention on a 16-section CT scanner (Aquilion 16; Toshiba Medical Systems, Tokyo, Japan) until September 2008 and on a 128-section CT scanner (Somatom Definition AS+, Siemens) thereafter. Approximately 20 sections were acquired parallel to the canthomeatal plane by using an incremental technique. STs were 4 and 6 mm in the skull base and cerebrum, respectively.

### Image Postprocessing

Postprocessing of the rotational image data to a volume dataset was performed by using a dedicated commercial software on a Leonardo medical workstation (InSpace 3D, Siemens). The software includes system-specific algorithms to correct beam hardening, scattered radiation, truncated projections, and ring artifacts. Reconstruction resulted in a volume dataset of approximately 400–500 sections with a 512 × 512 matrix. Single-section thickness was 0.2–0.3 mm (isotropic). For retrospective evaluation of ACT, data were further processed into 20 modified axial sections, parallel to the canthomeatal plane and analog to the conventional cranial MDCT (skull base ST, 4 mm;

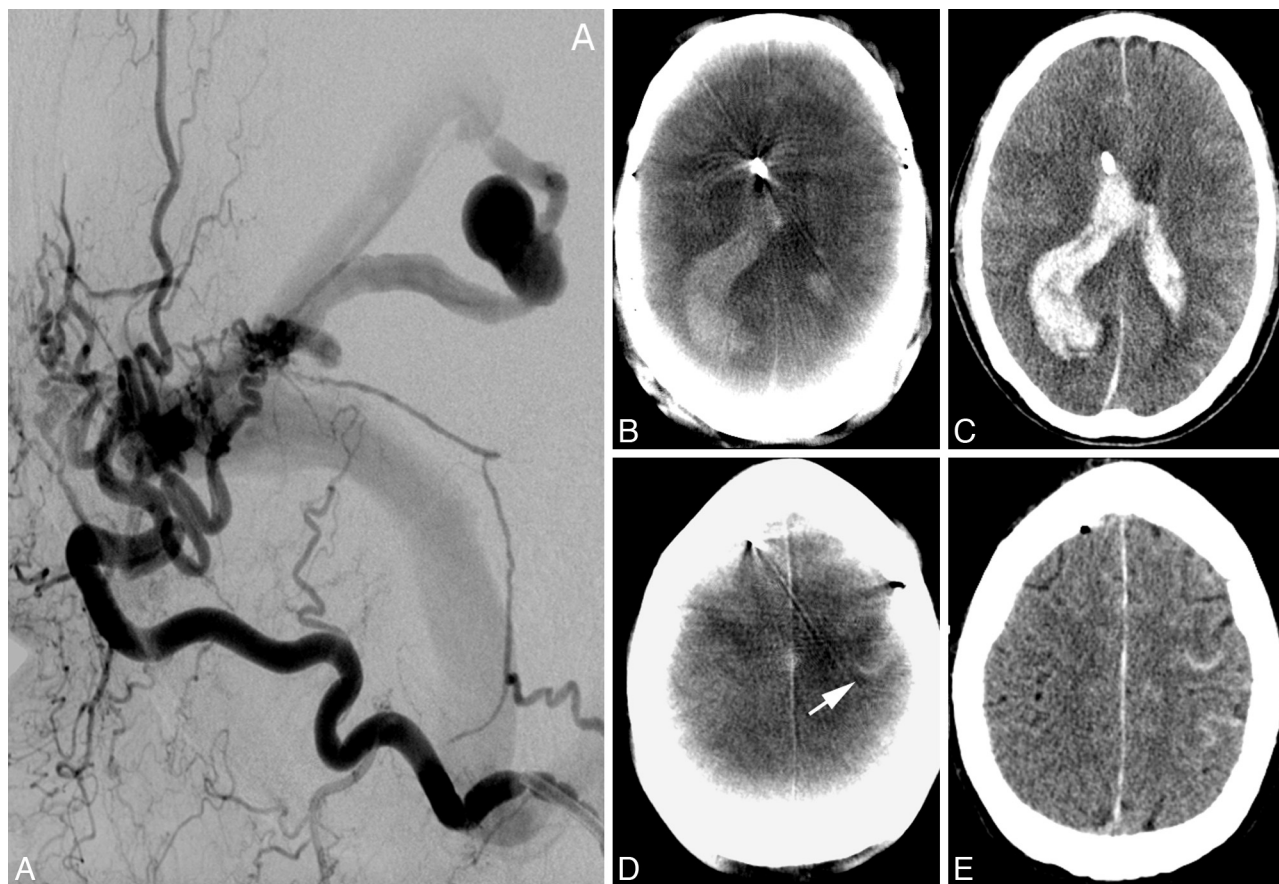


**Fig 2.** A 65-year-old man. A, Lateral occipital artery angiogram shows a tentorial dural fistula and a venous aneurysm. B–E, The ACT examination (B) after EVD application and diagnostic angiography depicts a large IVH and a small IPH of the right parietal lobe. Small amounts of SAH in a frontal sulcus on the left side can also be detected on the ACT examination (D, arrow). These findings can be confirmed on MDCT images (C and E). The exact position of EVD catheter tip can be accurately depicted on both examinations.

cerebrum ST, 6 mm). Window levels were not standardized, allowing the observers to choose their preferred window values on the PACS workstation. The images were anonymized, coded, and put in a PACS folder to be viewed under diagnostic conditions.

### Image Analysis and Statistics

Three neuroradiologists (M.K., J.-H.B., and A.X.), blinded to history, clinical symptoms, and acquisition technique, examined the datasets by using a PACS workstation (Centricity RA 1000; GE Healthcare, Milwaukee, Wisconsin). Two of the neuroradiologists (M.K., J.-H.B.) were very familiar with ACT examinations (>50 diagnosed ACTs), while the third (A.X.) was less experienced with this kind of procedure. Raters were asked to evaluate the examinations by using a scaled scoring system (0 = not identifiable; 1 = identifiable, but not diagnostic; and 2 = diagnostic) regarding anatomic structures and important pathologies relevant for the peri-interventional diagnosis: supra- or infratentorial ventricular system and supra- or infratentorial subarachnoid space; SAH, IPH, IVH; diagnostic evaluation of the basal ganglia and insular and central cortices; and location of the catheter tip (in case of EVD placement). Contingency tables and Wilcoxon signed ranks tests, to compare overall scores within categories, were calculated by using the Statistical Package for the Social Sciences 16 (SPSS; Chicago, Illinois). *P* values < .05 were considered statistically significant. Interobserver agreement was evaluated with weighted  $\kappa$  statistics, with a value above  $\kappa_w = 0.60$  representing substantial agreement.<sup>11</sup>

### Results

As expected, MDCT mostly scored diagnostic values in the evaluation of the various categories and was used as the criterion standard for the comparison with ACT. The results of all ratings are presented in On-line Table 1. Depicting the supratentorial ventricular system, ACT proved to be as reliable as MDCT, scoring a total of 94% of diagnostic values, 6% of identifiable values, and 0% of “not identifiable” scores (97.6%, 2.4%, and 0%, respectively, for MDCT; On-line Table 1). The Wilcoxon test showed no statistically significant difference between the 2 modalities in this category (*P* = .26). For example, in Fig 1D, we can diagnose the normal width of the supratentorial ventricular system on ACT. Both ACT (Fig 1D) and MDCT (Fig 1E) scans were assigned a diagnostic value in this case. In Fig 2B, the dilation of the supratentorial ventricular system due to IVH can be reliably detected on the ACT examination. In the evaluation of the supratentorial subarachnoid space, ACT proved to be diagnostic in 84.5% of cases (MDCT, 91.7%; *P* = .16). Sulcal effacement can be diagnosed without any problems on the ACT scan in Fig 2B. ACT scores are moderate regarding the analysis of the infratentorial ventricular system with 60.7% of “diagnostic” values, but only 3.6% of the cases were “not identifiable.” Also, regarding the infratentorial subarachnoid space the “diagnostic” values of ACT dropped further, being only 28.6% of the total, with 16.6% of the examinations tagged as “not identifiable” (Fig 3E). In



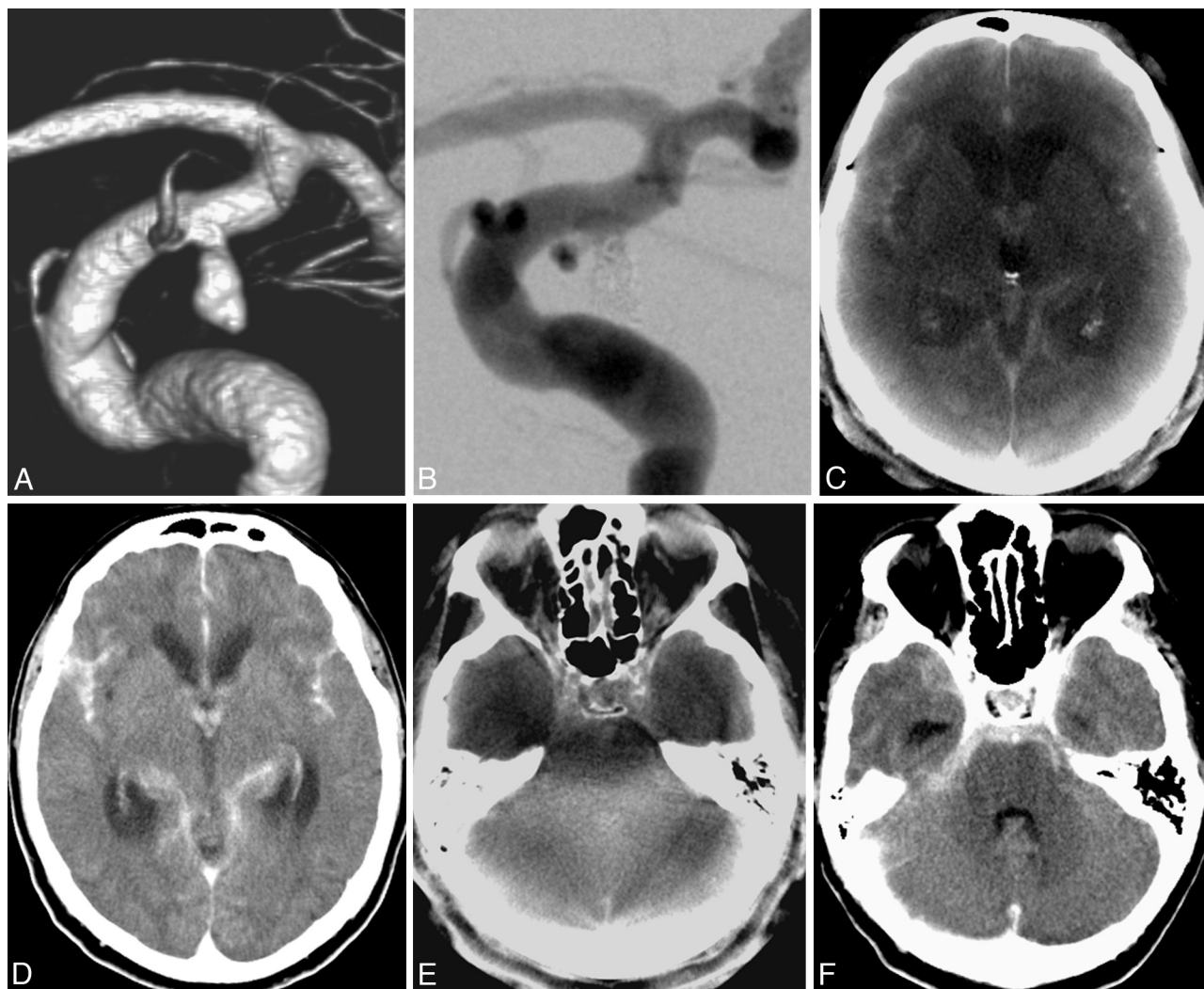


**Fig 3.** A, Ruptured distal carotid artery aneurysm of a 72-year-old man with acute SAH, Hunt and Hess 4. B, After endovascular treatment with Guglielmi detachable coils (Boston Scientific). C–F, ACT images (C and E) show the SAH and IVH as well as dilation of the supratentorial ventricular system. In contrast to MDCT (F), the fourth ventricle cannot be evaluated in the ACT examination (E) due to beam hardening artifacts. After implantation of a lumbar drain, follow-up MDCT scans (D and F) show a slight decrease of the lateral ventricle size.

comparison, MDCT scores for the infratentorial subarachnoidal space are, to a great extent, “diagnostic,” with 91.7% (Fig 3F).

ACT scored 90.3% of “diagnostic” values by the assessment of SAH, with the reviewers detecting 40 of the 41 SAHs seen in MDCT ( $P = .08$ , Figs 1 and 2D). In 3 cases, SAH could not be exactly quantified with ACT, thus scoring an “identifiable but not diagnostic” value. ACT produced similar results in the case of IPH and IVH, with 83.9% and 80% of “diagnostic” values, respectively (MDCT: 93.5% and 92%,  $P = .16$  and  $P = .11$ , Figs 2, 3). Twenty-nine of 31 IPHs and 24/25 IVHs could be depicted with ACT, proving a very good overall sensitivity for ICH. Three of the 41 SAHs and 2 of the 31 IPHs occurred during an intervention. All other hemorrhages occurred before treatment.

In the evaluation of gray matter, ACT scored very poor results: 17.8% for the basal ganglia, 44% for the insular cortex, and 13.1% for central cortex tagged as “not identifiable” ( $P < .05$  in all 3 categories). Less than 20% of ACTs were assigned a “diagnostic” value regarding all regions of gray matter tested. Especially the evaluation of the insular cortex is notably lim-

ited on ACTs due to ring artifacts (Fig 4C). In most cases, some regions of gray matter can be identified on ACT images, but reliable diagnosis of decreased attenuation or loss of gray-white borders is impossible.

Concerning the position of the EVD tip, there are no statistically significant differences between ACT and MDCT. With 97.1% of “diagnostic” values ( $P = .56$ ), ACT proved to be a reliable tool for the confirmation of correct catheter placement.

The results of  $\kappa$  statistics regarding the ratings among the categories are seen in the Table. All observers were controlled against each other regarding every method. Almost perfect agreement was documented among MDCT results ( $\kappa_w > 0.8$ ) and substantial agreement among ACT ratings ( $\kappa_w > 0.6$ ).

## Discussion

After neuroendovascular procedures and within the angiography suite, ACT provides cross-sectional CT-like images and enables an immediate detection of hemorrhage or hydrocephalus.<sup>1,2,10</sup> To the best of our knowledge, this is the largest retrospective study exploring the potential of ACT in the

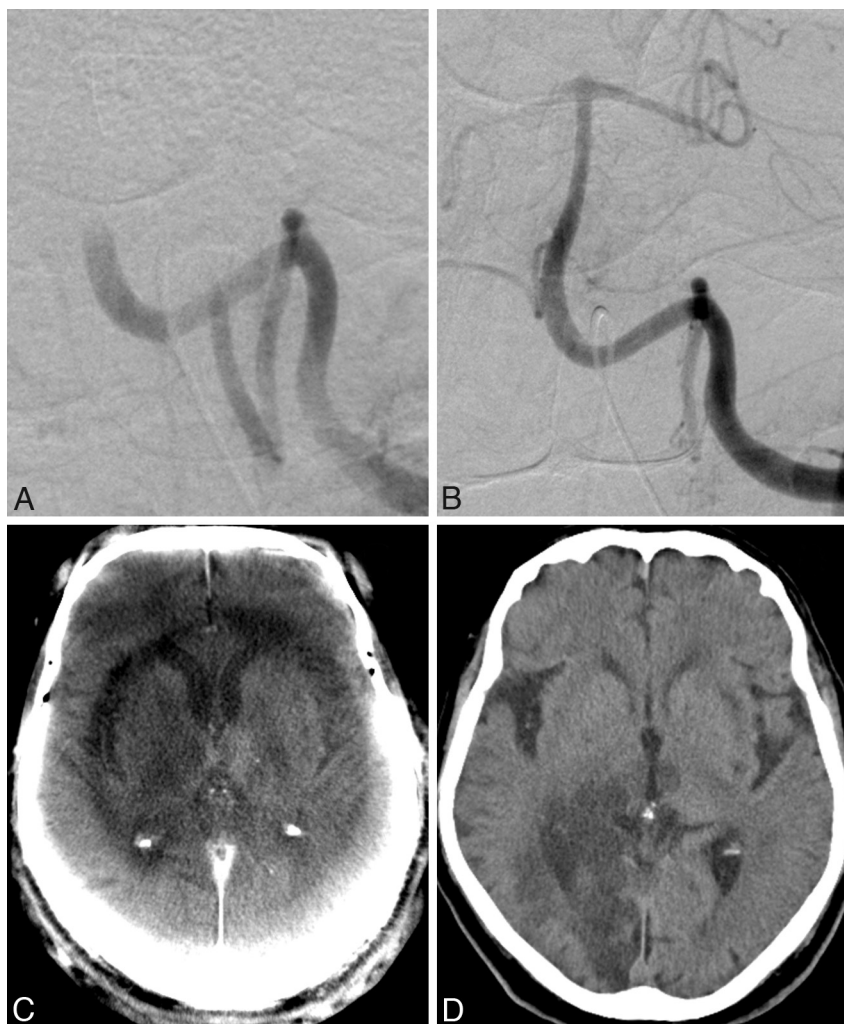


**Fig 4.** A, A 63-year-old woman with acute basilar artery thrombosis. B and C, After recanalization of the artery with a Penumbra System (Penumbra, Alameda, California) (B), an acute ischemic lesion of the right thalamus can be seen on the ACT images (C). There is no complication in the form of an IPH or SAH. Typical ring artifacts can be seen on ACT and should not be confused with areas of cerebral edema. D, The follow-up MDCT after 2 hours confirms the thalamic infarction but also depicts a right occipital lobe infarction, which was undetectable on the ACT examination.

Interobserver agreement		
	MDCT	ACT
Observer 1 vs 2	0.91	0.82
Observer 1 vs 3	0.87	0.72
Observer 2 vs 3	0.86	0.69
Mean $\kappa_w$	0.88	0.74

emergency diagnosis and the first evaluating the power of ACT in the detection of ischemic lesions.

In accordance with previous studies, in which ACT was proved to be as reliable as MDCT for the detection of ICH, in our collective experience, ACT showed no statistical significance in the evaluation of SAH, IPH, or IVH in comparison with MDCT. Most ratings regarding ACT were “diagnostic,” with 90.3%, 83.9%, and 80% for SAH, IPH, and IVH, respectively. As seen in Fig 1, after intracranial angioplasty and stent placement, a peri-interventional complication like SAH and subarachnoid contrast agent accumulation can be easily detected in the ACT image. This is 1 of the 5 cases in our series (3 SAHs, 2 IPHs) in which the hemorrhage occurred within the angiography suite during treatment. In such cases, detect-

ing the hemorrhage as soon as possible is crucial for the further management of the patient in the intensive care unit. Additionally, potentially dangerous transfer of the patient to the MDCT scanner would then not be necessary. Figure 2 shows an example in which ACT correctly depicts IPH and IVH after rupture of a venous aneurysm before treatment. Correct EVD placement can be verified in both examinations. In Fig 4, SAH and IVH, after rupture of an internal carotid artery aneurysm, can be accurately diagnosed in the ACT examination.

Regarding the ventricular system and the subarachnoid spaces, ACT also proved to be a reliable tool. For the infratentorial ventricular spaces, there are some limitations through beam hardening and bone-blooming artifacts; however, ACT can be compared with MDCT in the evaluation of these structures in the supratentorial compartment (Figs 1, 2, and 4).

Concerning the evaluation of gray matter and the detection of ischemic lesions, ACT was not reliable. Most scores on our study are “identifiable, but not diagnostic,” and there are a large number of examinations in which gray matter structures, like the basal ganglia or the insular cortex, are “not identifiable” at all. Acute ischemic lesions can hardly be detected in

ACT, and even bigger older lesions can be overlooked. As depicted in Fig 1, the patient has an older right frontal infarction, which can be easily detected in the MDCT examination but is practically undetectable in the ACT examination. In Fig 3, ACT shows a demarcated thalamic infarction, after recanalization of a basilar artery thrombosis. MDCT performed 2 hours later confirmed the thalamic infarction but, furthermore, depicted an acute large posterior cerebral artery territory infarction, whose early signs were undetectable in the ACT scan.

The position of the EVD catheter tip can be accurately determined with ACT. This feature is especially useful in cases of ruptured aneurysm and SAH. After placement of the EVD, the patient can be directly transferred to the angiography suite. The position of the EVD catheter tip can be verified within the angiography suite, before or after the diagnostic angiography or endovascular treatment of the ruptured aneurysm. Thus, precious time is saved, and the additional transfer of the patient to the MDCT scanner can be avoided.

Weighted  $\kappa$  statistics showed substantial agreement among ACT and perfect agreement among MDCT observer ratings. Because ACT provides us with cross-sectional CT-like images, even less experienced neuroradiologists (in our study, A.X.), however familiar with the interpretation of MDCT images, can successfully diagnose abnormalities in ACT examinations.

Contrary to other studies, we did not face any problems with motion artifacts in our patients because all patients had intubation narcosis before endovascular treatment.

Regarding the effective dose, the use of a 20-second ACT protocol in our study resulted in lower CTDI<sub>w</sub> values (manufacturer's information, ~35 mGy), as opposed to conventional cranial CT (reference value: CTDI<sub>w</sub> ~60 mGy).<sup>12</sup> This is still higher than that in the usual rotational angiography scans (5-second 3D-DSA, CTDI<sub>w</sub> ~9 mGy), but use of the 20-second protocol is necessary to achieve low-contrast resolution.<sup>13,14</sup> Contrary to Kyriakou et al,<sup>14</sup> who applied the high-dose ACT protocol (CTDI<sub>w</sub> ~75 mGy) in their study, we used the low-dose protocol solely for the purposes of our study.

An additional characteristic of ACT, which was not evaluated in our series but was very useful in the cases we treated with intracranial stent placement, is the depiction of small high-contrast objects like intracranial stents by means of ACT. With the same rotational dataset used in our study, we can produce thin cross-sectional images of <0.1-mm isotropic voxel size; these images have a quality superior to that of conventional MDCT or even DSA images.<sup>15-17</sup> This is a valuable

feature following intracranial angioplasty with stent placement because the same dataset, used to provide ACT images for the detection of hemorrhage, can be used to depict deployment characteristics and stent conformability (Fig 1).

## Conclusions

ACT is a very useful tool in peri-interventional diagnosis. In our study, ACT was as good as MDCT for the detection or exclusion of ICH and hydrocephalus or verification of correct EVD placement during or after neurointervention. However, ACT is currently not reliable in depicting ischemic lesions.

## References

1. Heran NS, Song JK, Namba K, et al. The utility of DynaCT in neuroendovascular procedures. *AJNR Am J Neuroradiol* 2006;27:330-32
2. Doelken M, Struffert T, Richter G, et al. Flat-panel detector volumetric CT for visualization of subarachnoid hemorrhage and ventricles: preliminary results compared to conventional CT. *Neuroradiology* 2008;50:517-23
3. Kalender WA. The use of flat-panel detectors for CT imaging [in German]. *Radiologe* 2003;43:379-87
4. Loose R, Wucherer M, Brunner T, et al. Visualization of 3D low contrast objects by CT cone-beam reconstruction of a rotational angiography with a dynamic solid body detector [in German]. *Rofo* 2005;S1:PO160
5. Groh BA, Siewerdsen JH, Drake DG, et al. A performance comparison of flat panel imager-based MV and kV cone-beam CT. *Med Phys* 2002;29:967-75
6. Daly MJ, Siewerdsen JH, Moseley D, et al. Intraoperative cone-beam CT for guidance of head and neck surgery: assessment of dose and image quality using a C-arm prototype. *Med Phys* 2006;33:3767-807
7. Kalender WA, Kyriakou Y. Flat-detector computed tomography (FD-CT). *Eur Radiol* 2007;17:2767-79
8. Buhk JH, Kallenberg K, Mohr A, et al. Evaluation of angiographic computed tomography in the follow-up after endovascular treatment of cerebral aneurysms: a comparative study with DSA and TOF-MRA. *Eur Radiol* 2009;19:430-36
9. Buhk JH, Lingor P, Knauth M. Angiographic CT with intravenous administration of contrast medium is a noninvasive option for follow-up after intracranial stenting. *Neuroradiology* 2008;50:349-54
10. Struffert T, Richter G, Engelhorn T, et al. Visualisation of intracerebral haemorrhage with flat-detector CT compared to multislice CT: results in 44 cases. *Eur Radiol* 2009;19:619-25
11. Cohen J. Weighted kappa: nominal scale agreement with provision for scaled disagreement or partial credit. *Psychol Bull* 1968;70:213-20
12. Bundesamt fuer Strahlenschutz. Diagnostische Referenzwerte fuer radiologische Untersuchungen. *Bundesanzeiger* 2003;143:17503-10
13. Schueler BA, Kallmes DF, Cloft HJ. 3D cerebral angiography: radiation dose comparison with digital subtraction angiography. *AJNR Am J Neuroradiol* 2005;26:1898-901
14. Kyriakou Y, Richter G, Dörfler A, et al. Neuroradiologic applications with routine C-arm flat panel detector CT: evaluation of patient dose measurements. *AJNR Am J Neuroradiol* 2008;29:1930-36
15. Richter G, Engelhorn T, Struffert T, et al. Flat panel detector angiographic CT for stent-assisted coil embolization of broad-based cerebral aneurysms. *AJNR Am J Neuroradiol* 2007;10:1902-08
16. Ebrahimi N, Claus B, Lee CY, et al. Stent conformity in curved vascular models with simulated aneurysm necks using flat-panel CT: an in vitro study. *AJNR Am J Neuroradiol* 2007;28:823-29
17. Benndorf G, Strother CM, Claus B, et al. Angiographic CT in cerebrovascular stenting. *AJNR Am J Neuroradiol* 2005;26:1813-8